# Syntheses, Molecular Structures, and Countercation-Induced Structural Transformation of Monomeric $\alpha$-Keggin-Type Polyoxotungstate-Coordinated Mono- and Dipalladium(II) Complexes

# Syntheses, Molecular Structures, and Countercation-induced Structural Transformation of Monomeric α-Keggin-type Polyoxotungstate-coordinated Mono- and Dipalladium(II) Complexes

Chika Nozaki Kato,*[a,b] Ippo Nakahira,[a] Ryota Kasai,[a] and Shigeki Mori[c]

---

[a] Dr. C. N. Kato, I. Nakahira, R. Kasai

Department of Chemistry, Faculty of Science, Shizuoka University, 836 Ohya, Suruga-ku, Shizuoka 422-8529, Japan

E-mail: kato.chika@shizuoka.ac.jp

https://wwp.shizuoka.ac.jp/katolab/

[b] Dr. C. N. Kato

Research Institute of Green Science and Technology, Shizuoka University, 836 Ohya, Suruga-ku, Shizuoka 422-8529, Japan

[c] Dr. S. Mori

Advanced Research Support Center, Ehime University, Matsuyama 790-8577, Japan

**Abstract:** Monomeric α-Keggin-type polyoxotungstate-coordinated mono- and di-palladium(II) complexes, i.e., $Cs_5[\alpha\text{-}PW_{11}O_{39}\{Pd^{II}(Me_2ppz)\}]\cdot 5H_2O$ (**Cs-1**) ($Me_2ppz$ = *N,N'*-dimethylpiperazine), $[(CH_3)_4N]_4H[\alpha\text{-}PW_{11}O_{39}\{Pd^{II}(Me_2ppz)\}]\cdot 8H_2O$ (**TMA-1**), and $Cs_{2.5}H_{0.5}[\alpha\text{-}PW_{11}O_{39}\{Pd^{II}(en)\}_2]\cdot 7H_2O$ (en = ethylenediamine) (**Cs-2**), were synthesized by 1:1 or 1:2 stoichiometric reactions of mono-lacunary α-Keggin polyoxotungstate $[\alpha\text{-}PW_{11}O_{39}]^{7-}$ with $PdCl_2(Me_2ppz)$ and $PdCl_2(en)$ in aqueous solution. Subsequent purification from water afforded these compounds as analytically pure homogeneous yellow precipitates. Single-crystal X-ray structural analysis of **Cs-1** revealed that a palladium(II) moiety, i.e., $[Pd(Me_2ppz)]^{2+}$, was coordinated to two oxygen atoms in the mono-vacant site of $[PW_{11}O_{39}]^{7-}$ with an asymmetric configuration, resulting in an overall $C_1$ symmetry. With regard to the crystal structure of **Cs-2**, two palladium species of the $[Pd(en)]^{2+}$ type were coordinated to two oxygen atoms in the mono-vacant site with symmetric configuration, resulting in an overall $C_s$ symmetry. A unique structural transformation of the mono-lacunary α-Keggin structure of **Cs-1** to the di-lacunary γ-Keggin polyoxotungstate $Cs_7[\gamma\text{-}PW_{10}O_{36}]$ was observed upon the addition of cesium chloride.

**Keywords:** polyoxometalate; palladium; molecular structure; structural transformation

# Introduction

Palladium-containing polyoxometalates (POMs) have attracted much attention due to the fact that the incorporation of noble metal ions and their derivatives into completely inorganic, thermally stable, and redox-stable POM frameworks may allow for the stabilization of noble metal sites as well as the solubilization in aqueous and organic media.[1,2] Various palladium-containing POMs have been reported;[2] however, only in few cases their structure was determined by X-ray crystallography structural analysis. Some recent examples include $[Se^{IV}_2Pd^{II}_4W^{VI}_{14}O_{56}H]^{11-}$,[3] $[Se^{IV}_4Pd^{II}_4W^{VI}_{28}O_{108}H_{12}]^{12-}$,[3] $[Pd^{II}_4(\alpha\text{-}P_2W_{15}O_{56})_2]^{16-}$,[4] $[Pd^{II}_3(TeW_9O_{33})_2]^{10-}$,[5] $[\gamma\text{-}H_2SiW_{10}O_{36}Pd^{II}_2(OAc)_2]^{4-}$,[6] and $[\{(\gamma\text{-}H_2SiW_{10}O_{36}Pd^{II}_2)(O_2C(CH_2)_nCO_2)\}]$ ($n$ = 1,3, and 5).[7]

In this study, we successfully obtained the cesium and tetramethylammonium salts $Cs_5[\alpha\text{-}PW_{11}O_{39}\{Pd^{II}(Me_2ppz)\}]\cdot5H_2O$ (Me$_2$ppz = $N,N'$-dimethylpiperazine) (**Cs-1**) and $[(CH_3)_4N]_4H[\alpha\text{-}PW_{11}O_{39}\{Pd^{II}(Me_2ppz)\}]\cdot8H_2O$ (**TMA-1**), along with $Cs_{2.5}H_{0.5}[\alpha\text{-}PW_{11}O_{39}\{Pd^{II}(en)\}_2]\cdot7H_2O$ (en = ethylenediamine) (**Cs-2**). In particular, compounds **Cs-1** and **Cs-2** were obtained in the form of crystals (i.e., suitable for X-ray structural analysis) by slow evaporation from water. The X-ray crystal structure of **Cs-1** revealed that the *cis*-palladium(II) moiety was coordinated to the two oxygen atoms in the mono-vacant site of $[\alpha\text{-}PW_{11}O_{39}]^{7-}$ with an asymmetric configuration, resulting in an overall $C_1$ symmetry. In the case of **Cs-2**, the two *cis*-palladium(II) moieties were coordinated to two oxygen atoms, resulting in an overall $C_s$ symmetry. Compounds **Cs-1**, **TMA-1**, and **Cs-2** were characterized by X-ray crystallography, elemental analysis, thermogravimetric/differential thermal analysis (TG/DTA), as well as Fourier transform infrared (FTIR), ultraviolet-visible (UV-Vis), and solution {$^1$H, $^{13}$C, $^{31}$P, and $^{183}$W} nuclear magnetic resonance (NMR) spectroscopy.

The structural transformation of the mono-lacunary α-Keggin structure of **Cs-1** to a di-lacunary γ-Keggin polyoxotungstate, i.e., $Cs_7[\gamma\text{-PW}_{10}O_{36}]$, upon addition of cesium chloride was also described.

## Results and Discussion

**Syntheses and characterization of Cs-1, TMA-1, and Cs-2**

The cesium and tetramethylammonium salts of $[\alpha\text{-PW}_{11}O_{39}\{Pd^{II}(Me_2ppz)\}]^{5-}$ (**1**) were easily formed by a 1:1 stoichiometric reaction between $Pd^{II}Cl_2(Me_2ppz)$ and mono-lacunary α-Keggin POM $[\alpha\text{-PW}_{11}O_{39}]^{7-}$ in an aqueous solution at 25 °C in air. While the cesium salt of **1** could be obtained upon addition of cesium chloride (10 mmol) to a mixture of $Pd^{II}Cl_2(Me_2ppz)$ (0.4 mmol) and mono-lacunary Keggin POM $[\alpha\text{-PW}_{11}O_{39}]^{7-}$ (0.4 mmol), a small amount of $Cs_7[\gamma\text{-PW}_{10}O_{36}]^{[8,9]}$ was also generated as by-product. In order to isolate the target product, it was necessary to remove the white powder constituted of $Cs_7[\gamma\text{-PW}_{10}O_{36}]$ by ice-cooling the aqueous solution in which the crude precipitate was dissolved. Compound **Cs-1** was finally isolated as an analytically pure, yellow crystalline powder in 37% yield. Reducing the amount of cesium chloride to suppress the $Cs_7[\gamma\text{-PW}_{10}O_{36}]$ by-production led to a significantly decreased yield of **Cs-1** (e.g., the addition of 7.5 mmol of cesium chloride resulted in a yield of 24%). A single crystal of **Cs-1** was obtained for X-ray crystallography by slow evaporation from an aqueous solution containing the purified powder. The tetramethylammonium salt of **1** was also obtained upon addition of tetramethylammonium chloride to the mixture. In the case of **TMA-1**, the formation of by-products was not observed even when the amount of tetramethylammonium chloride was changed. The purification was performed by reprecipitation from water. Compound **TMA-1** was also obtained as an analytically pure, yellow powder in 23% yield. Single crystals of **TMA-1** suitable for X-ray structural analysis

could neither be obtained by slow evaporation from water nor vapor diffusion from water/methanol and water/ethanol.

The cesium salt of $[\alpha\text{-PW}_{11}\text{O}_{39}\{\text{Pd}^{II}(\text{en})\}_2]^{3-}$ (**2**) was obtained by a 2:1 stoichiometric reaction between $\text{PdCl}_2(\text{en})$ and $[\alpha\text{-PW}_{11}\text{O}_{39}]^{7-}$ in an aqueous solution at 25 °C in air. The cesium salt of **2** was obtained upon addition of cesium chloride to a mixture of $\text{PdCl}_2(\text{en})$ and mono-lacunary Keggin POM, followed by precipitation from water. In the case of **Cs-2**, no by-product formation was observed due to the amount of cesium chloride. Compound **Cs-2** was finally isolated as an analytically pure, yellow crystalline powder in 30% yield. A single crystal of **Cs-2** for X-ray crystallography was obtained by slow evaporation from an aqueous solution containing the purified crystalline powder.

The elemental analysis and TG/DTA results (Figs. S1–S3) were in good agreement with the calculated values based on the chemical formulas of **Cs-1**, **TMA-1**, and **Cs-2** (see Experimental). The analytical value of potassium was less than 0.1%, indicating that these palladium compounds did not contain potassium ions.

For the X-ray crystal structure analysis of **Cs-1**, polyoxoanion **1** was observed as two molecules, i.e., Units A and A', as shown in Fig. S4. They possessed the same molecular structure in which one palladium species, i.e., $[\text{Pd}(\text{Me}_2\text{ppz})]^{2+}$, was coordinated to two oxygen atoms in a mono-vacant site of $[\alpha\text{-PW}_{11}\text{O}_{39}]^{7-}$, resulting in an overall $C_1$ symmetry. Units A and A' are shown in Figs. 1 and S5, respectively. Thus, polyoxoanion **1** was chiral; however, Unit A formed an enantiomer with Unit B that appeared by symmetry operation (Unit A' also formed an enantiomer with Unit B'), as shown in Fig. S4. Since Units A and B (or Units A' and B') were present in equal amounts, they were a racemic mixture. Selected bond lengths and angles around the palladium centers are summarized in Tables 1 and S1, while other bond lengths (Å) and angles (°) (Tables S2 and S3) as well as the bond valence sum (BVS) calculations of the W, P, and O atoms (Tables S4 and S5) are given in the Supporting Information.

The Pd(1)–O(3)–W(1) and Pd(1)–O(11)–W(5) bond angles in Unit A were 172.2(10)° and 148.9(8)°, respectively, which were remarkably tilted towards the other two terminal oxygen

atoms at the mono-vacant site, as shown in Fig. 2(a). A similar tendency was observed in Unit A'. However, the distances between the hydrogen atoms of the Me2ppz molecule and the terminal oxygen atoms O(5) and O(10) were long, and no clear interaction was confirmed between them.

The bond valence sums (BVSs)[10–14] which were calculated on the basis of the observed bond lengths for Units A and A', were in the range of 5.941–6.352 (average 6.09) and 5.999–6.562 (average 6.17) for the 11 W atoms, 4.940 and 4.970 for the internal P atom, as well as 1.562–2.107 (average 1.88) and 1.698–2.078 (average 1.89) for the 39 oxygen atoms in the Keggin unit. These values reasonably corresponded to the formal valences of $W^{6+}$, $P^{5+}$, and $O^{2-}$. When two equivalents of $Pd^{II}Cl_2(Me_2ppz)$ were reacted with $[\alpha\text{-}PW_{11}O_{39}]^{7-}$ under the same conditions, di-palladium species were not formed.

The molecular structure of **Cs-2** is illustrated in Fig. 3. Selected bond lengths and angles around the palladium centers are summarized in Table 2, while other bond lengths (Å) and angles (°) (Table S6) as well as the bond valence sum (BVS) calculations of the W, P, and O atoms (Table S7) are also given in the Supporting Information.

Single-crystal X-ray structural analysis of **Cs-2** revealed that two palladium species of the $[Pd(en)]^{2+}$ type were coordinated to two oxygen atoms in a mono-vacant site of $[\alpha\text{-}PW_{11}O_{39}]^{7-}$ with a symmetric configuration, which resulted in an overall $C_s$ symmetry. The W(1)–O(3)–Pd(1) and W(2)–O(6)–Pd(2) bond angles were 155.0(5)° and 149.4(5)°, respectively, and were bent outward from each other (Fig. 2(b)). The Pd⋯Pd distance was 3.543 Å, which was larger than those of $K_9[Pd_2(\alpha\text{-}PW_{11}O_{39}H_{0.5})_2]\cdot37H_2O$ (3.015(5) Å), $K_{14}Li[anti\text{-}Pd_2(\alpha_2\text{-}P_2W_{17}O_{61}H_{0.5})_2]\cdot50H_2O$ (3.000(4) Å), and $K_{10}[syn\text{-}Pd_2(\alpha_2\text{-}P_2W_{17}O_{61}H_3)_2]\cdot50H_2O$ (3.051(5) Å).[1]

The bond valence sums (BVSs), which were calculated on the basis of the observed bond lengths of **Cs-2**, were in the range of 6.054 – 6.246 (average 6.18) for the 11 W atoms, 4.884 for the internal P atom, and 1.687 – 2.137 (average 1.97) for the 39 oxygen atoms in the Keggin unit. These values reasonably corresponded to the formal valences of $W^{6+}$, $P^{5+}$, and $O^{2-}$. It was not possible to determine the position of 0.5 protons from the BVS value of oxygen. In the case

of a 1:1 reaction between PdCl$_2$(en) and [$\alpha$-PW$_{11}$O$_{39}$]$^{7-}$ under the same conditions, mono-palladium species were not formed.

Table 1. Selected bond lengths (Å) and angles (°) around a palladium site in Unit A of **Cs-1**

| Lengths (Å) | | | |
|---|---|---|---|
| W(1)-O(3) | 1.787(16) | N(1)-C(1) | 1.46(3) |
| W(2)-O(5) | 1.731(19) | N(1)-C(2) | 1.50(3) |
| W(5)-O(11) | 1.793(15) | N(1)-C(3) | 1.50(3) |
| W(6)-O(10) | 1.733(15) | Average | 1.49 |
| Average | 1.761 | N(2)-C(4) | 1.53(3) |
| W(1)-O(4) | 1.930(17) | N(2)-C(5) | 1.51(3) |
| W(2)-O(4) | 1.868(17) | N(2)-C(6) | 1.42(3) |
| W(5)-O(19) | 1.911(18) | Average | 1.49 |
| W(6)-O(19) | 1.920(18) | C(2)-C(4) | 1.51(3) |
| Average | 1.907 | C(3)-C(5) | 1.50(3) |
| Pd(1)-O(3) | 1.982(16) | Average | 1.51 |
| Pd(1)-O(11) | 2.006(15) | | |
| Average | 1.994 | | |
| Pd(1)-N(1) | 2.020(19) | | |
| Pd(1)-N(2) | 2.002(18) | | |
| Average | 2.011 | | |

| Angles (º) | | | |
|---|---|---|---|
| Pd(1)-O(3)-W(1) | 172.2(10) | C(1)-N(1)-C(2) | 113.6(18) |
| Pd(1)-O(11)-W(5) | 148.9(8) | C(1)-N(1)-C(3) | 108.2(18) |
| Average | 160.6 | C(2)-N(1)-C(3) | 106.1(17) |
| O(3)-Pd(1)-O(11) | 90.5(6) | Average | 109.3 |
| O(3)-Pd(1)-N(2) | 98.0(7) | C(4)-N(2)-C(5) | 107.8(17) |
| O(11)-Pd(1)-N(1) | 96.7(7) | C(4)-N(2)-C(6) | 110.3(19) |
| N(1)-Pd(1)-N(2) | 74.5(8) | C(5)-N(2)-C(6) | 111(2) |
| Average | 89.9 | Average | 110 |
| Pd(1)-N(1)-C(1) | 122.4(14) | N(1)-C(2)-C(4) | 108.7(19) |
| Pd(1)-N(1)-C(2) | 102.9(14) | N(1)-C(3)-C(5) | 109.6(18) |
| Pd(1)-N(1)-C(3) | 102.1(13) | N(2)-C(4)-C(2) | 107.0(19) |
| Pd(1)-N(2)-C(4) | 102.3(14) | N(2)-C(5)-C(3) | 106.7(18) |
| Pd(1)-N(2)-C(5) | 103.1(13) | Average | 108.0 |
| Pd(1)-N(2)-C(6) | 121.8(16) | W(1)-O(4)-W(2) | 145.4(10) |
| Average | 109.1 | W(5)-O(19)-W(6) | 122.3(9) |
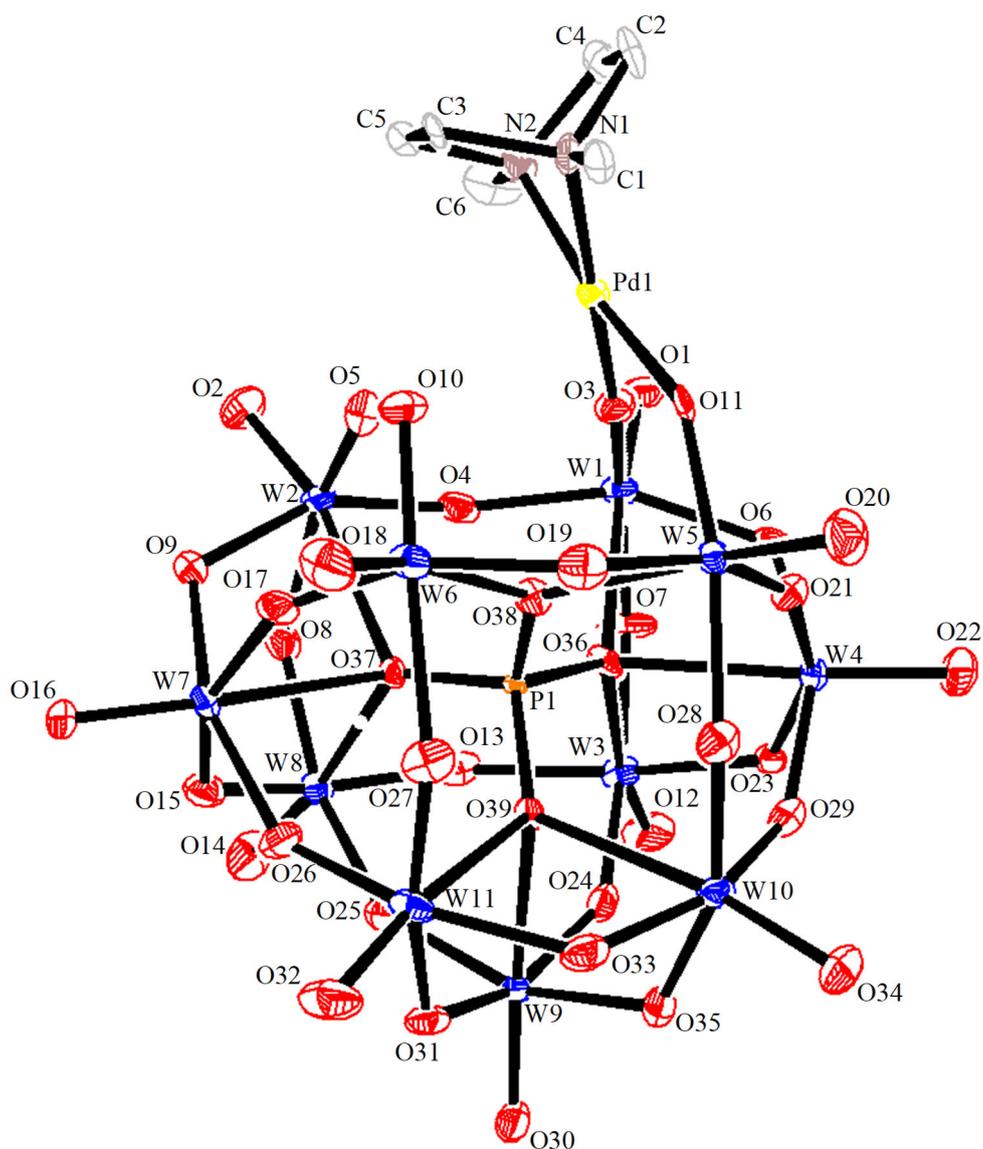
Figure 1. Molecular structure (ORTEP drawing) of $[\alpha\text{-}PW_{11}O_{39}\{Pd^{II}(Me_2ppz)\}]^{5-}$ (**1**). Polyoxoanion **1** was observed as two molecules named Unit A and A', as shown in Fig. S4. In this figure, the molecular structure of unit A is depicted. The W, O, P, Pd, C, and N atoms are represented by blue, red, orange, yellow, gray and pink colors, respectively.
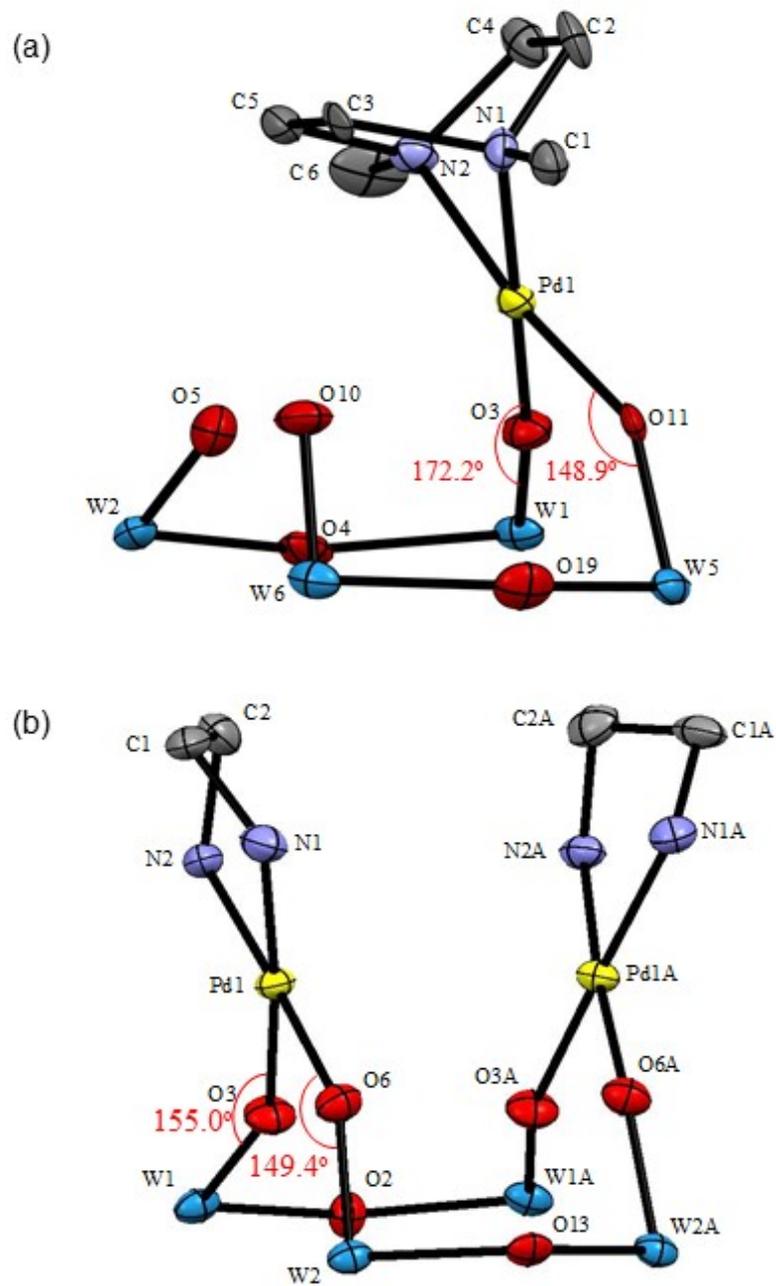
Figure 2. Partial structures around the palladium sites in (a) **Cs-1** (Unit A) and (b) **Cs-2**.

Table 2. Selected bond lengths (Å) and angles (°) around two palladium sites in **Cs-2**

| Lengths (Å) | | | |
|---|---|---|---|
| Pd(1)-O(3) | 1.994(8) | W(1)-O(3) | 1.753(8) |
| Pd(1)-O(6) | 2.011(8) | W(2)-O(6) | 1.766(8) |
| Average | 2.003 | Average | 1.756 |
| Pd(1)-N(1) | 2.007(10) | W(1)-O(2) | 1.907(3) |
| Pd(1)-N(2) | 1.991(10) | W(2)-O(13) | 1.924(5) |
| Average | 1.999 | Average | 1.919 |
| N(1)-C(1) | 1.456(16) | C(1)-C(2) | 1.522(19) |
| N(2)-C(2) | 1.476(14) | | |
| Average | 1.466 | | |
| | | Pd(1)···Pd(1A) | 3.543 |
| Angles (º) | | | |
| W(1)-O(3)-Pd(1) | 155.0(5) | O(3)-Pd(1)-O(6) | 92.4(3) |
| W(2)-O(6)-Pd(1) | 149.4(5) | O(6)-Pd(1)-N(1) | 92.6(4) |
| Average | 146.0 | O(3)-Pd(1)-N(2) | 90.5(4) |
| O(3)-Pd(1)-N(1) | 173.8(4) | N(1)-Pd(1)-N(2) | 84.3(4) |
| O(6)-Pd(1)-N(2) | 175.7(4) | Average | 90.0 |
| Average | 174.8 | | |
| Pd(1)-N(1)-C(1) | 109.5(8) | N(1)-C(1)-C(2) | 108.2(10) |
| Pd(1)-N(2)-C(2) | 109.3(8) | N(2)-C(2)-C(1) | 106.2(10) |
| W(1)-O(2)-W(1A) | 145.0(6) | W(2)-O(13)-W(2A) | 121.6(6) |
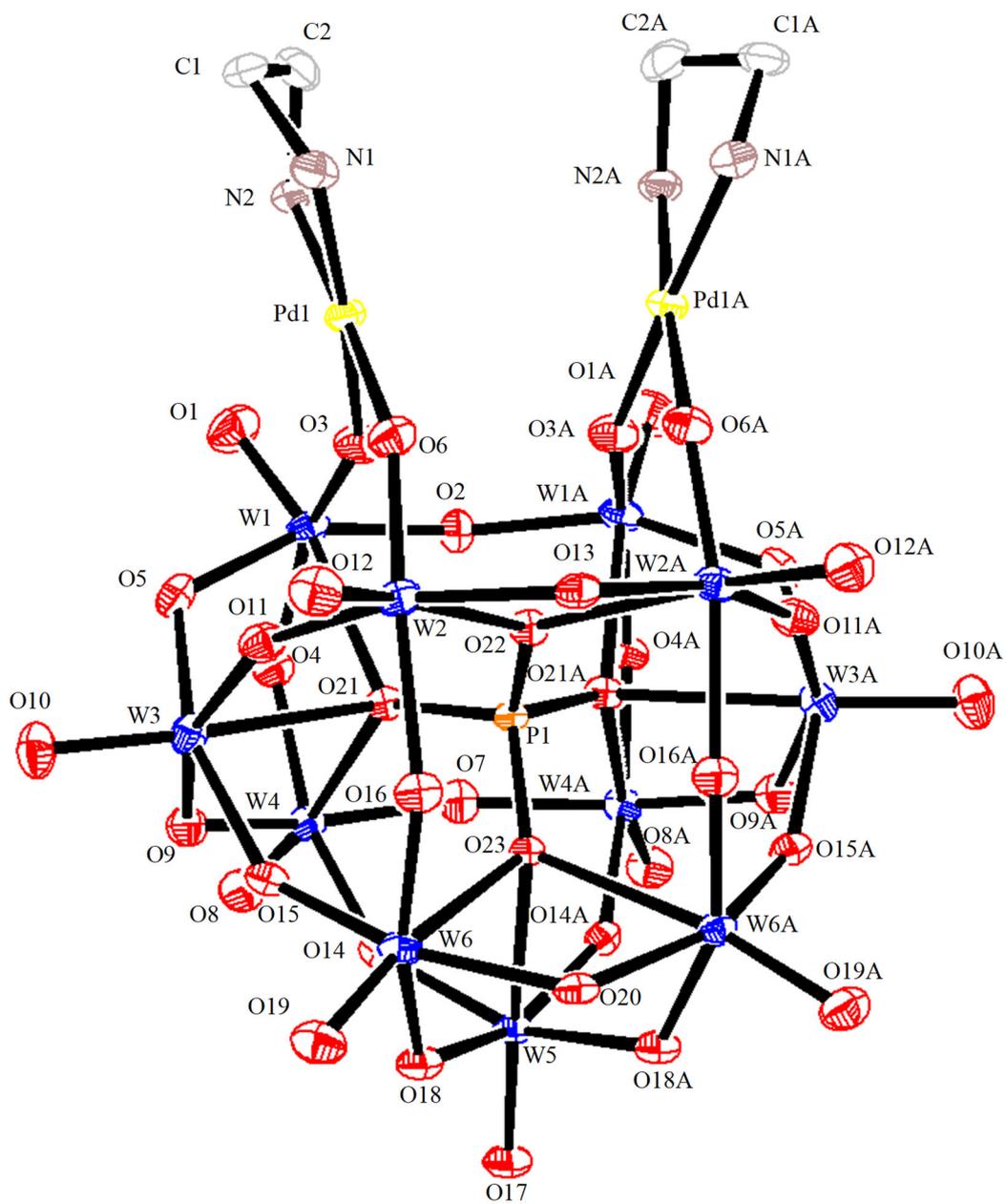
Figure 3. Molecular structure (ORTEP drawing) of $[\alpha\text{-PW}_{11}\text{O}_{39}\{\text{Pd}^{\text{II}}(\text{en})\}_2]^{3-}$ (**2**). The W, O, P, Pd, C, and N atoms are represented by blue, red, orange, yellow, gray and pink colors, respectively.

The FTIR spectrum of **Cs-1** in the polyoxometalate region (1200 – 400 cm$^{-1}$) was measured in a KBr disk, as shown in Fig. 4a. The spectral pattern of **Cs-1** (1092, 1042, 948, 895, 859, 807, 792, 757, 723, and 508 cm$^{-1}$) was different from that of $K_7[\alpha\text{-PW}_{11}O_{39}]\cdot13H_2O$ (1086, 1043, 953, 903, 862, 810, and 734 cm$^{-1}$),[15,16] suggesting that $[Pd(Me_2ppz)]^{2+}$ was coordinated to the vacant site of $[\alpha\text{-PW}_{11}O_{39}]^{7-}$. The spectral pattern of **TMA-1** (1084, 1045, 950, 890, 849, 806, 794, 761, 731, and 512 cm$^{-1}$) was similar to that of **Cs-1**, as shown in Fig. 4b. The 1457 cm$^{-1}$ band in the case of **Cs-1** as well as the bands at 1485, 1453, and 1383 cm$^{-1}$ for **TMA-1** were due to the Me$_2$ppz molecule and tetramethylammonium ions. The FTIR spectrum of **Cs-2** exhibited bands at 1098, 1048, 976, 952, 892, 852, 796, 735, and 551 cm$^{-1}$ (Fig. 4c), which were also different from those of $K_7[\alpha\text{-PW}_{11}O_{39}]\cdot13H_2O$. This suggested that $[Pd(en)]^{2+}$ was coordinated to the vacant site of $[\alpha\text{-PW}_{11}O_{39}]^{7-}$. The bands at 1454, 1396, 1363, 1312, 1293, 1165, and 1154 cm$^{-1}$ were attributed to the ethylenediamine molecules.

The $^{31}P$ NMR spectrum of **Cs-1** in $D_2O$ displayed a clear single-line spectrum at $-11.39$ ppm due to the internal phosphorus atom, confirming the purity and homogeneity of the sample (Fig. 5a). The signal was shifted compared with that of $K_7[\alpha\text{-PW}_{11}O_{39}]\cdot13H_2O$ ($\delta -10.67$). A single-line spectrum was also observed for **TMA-1** in $D_2O$ (Fig. 5b), which consisted of a signal at $-11.80$ ppm that was slightly shifted compared to that of **Cs-1**. However, the $^{31}P$ NMR spectrum of a mixture of **Cs-1** and **TMA-1** in $D_2O$ showed a single signal, confirming that **Cs-1** and **TMA-1** featured the same polyoxoanion **1**. For **Cs-2**, no signal was observed in the $^{31}P$ NMR spectrum measured in $D_2O$ because of its low solubility in water. Attempts were made to improve the solubility of **2** by preparing the potassium salt; however, no improvement in water solubility was observed. In attempts to prepare the sodium and lithium salts, the use of their chlorides, perchlorates, and nitrates caused the formation of PdCl$_2$(en). In the $^{31}P$ NMR spectrum of **Cs-2** measured in DMSO-$d_6$, a signal was observed at $-12.42$ ppm (Fig. 6), which was shifted relative to that of $K_7[\alpha\text{-PW}_{11}O_{39}]\cdot13H_2O$ ($\delta -10.12$) observed in DMSO-$d_6$.
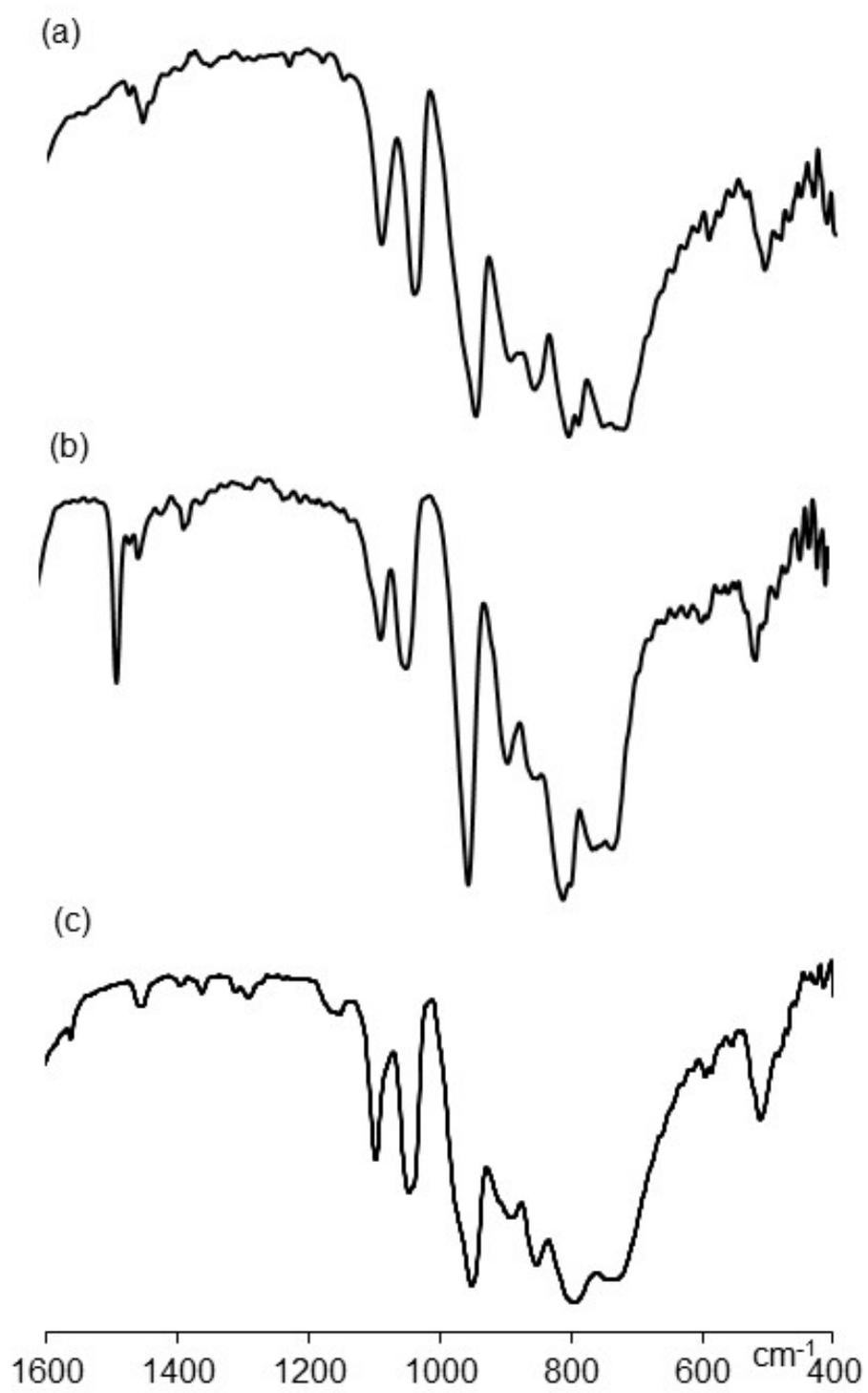
Figure 4. FT-IR spectra (as KBr disks) of (a) **Cs-1**, (b) **TMA-1**, and (c) **Cs-2**
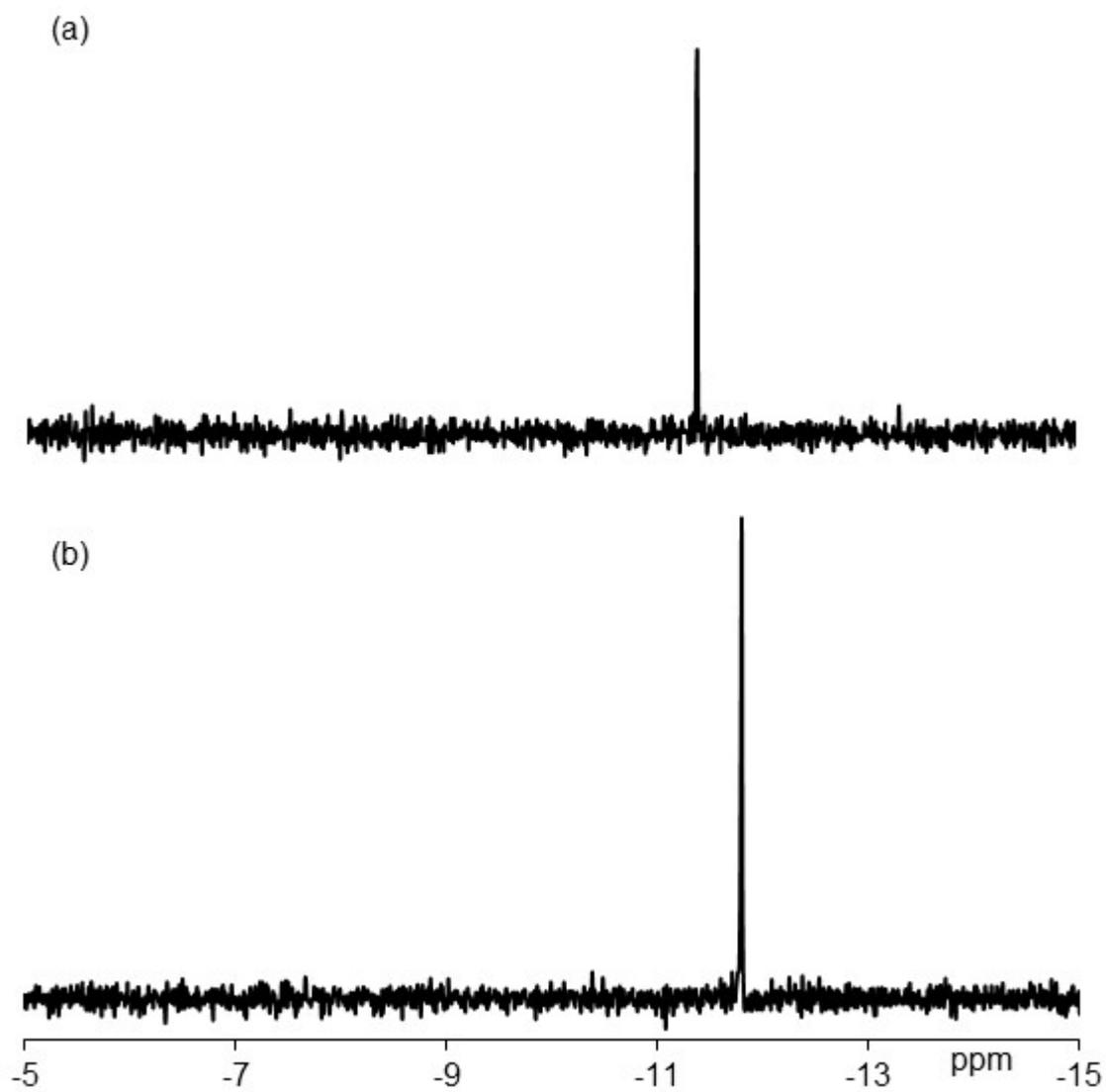
Figure 5. $^{31}$P NMR spectra in D$_2$O of (a) **Cs-1** and (b) **TMA-1**
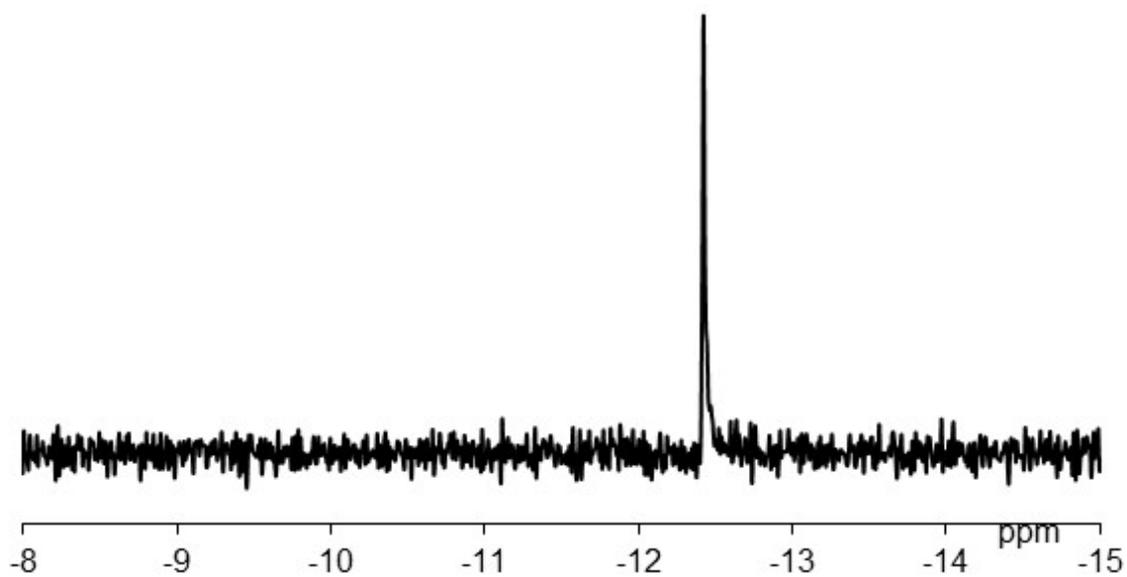
Figure 6. $^{31}$P NMR spectrum of **Cs-2** in DMSO-$d_6$
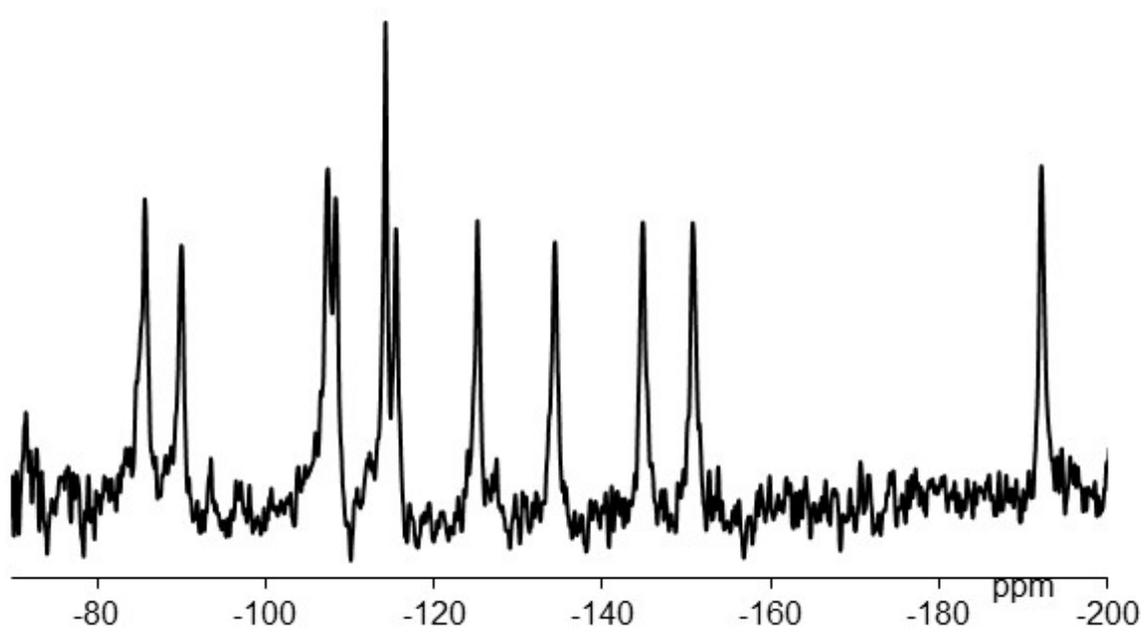
Figure 7. $^{183}$W NMR spectrum in D$_2$O of the potassium salt of **1**.

The preparation of potassium salt of **1** is shown in Experimental Section.

The $^{183}$W NMR spectrum in D$_2$O of the potassium salt of **1** obtained upon addition of an excess of KCl instead of cesium or tetramethylammonium chloride exhibited 11 signals at −85.7, −90.0, −107.4, −108.3, −114.3, −115.5, −125.2, −134.4, −144.8, −150.7, and −192.1 ppm with approximately 1:1:1:1:1:1:1:1:1:1:1 intensities; this indicates that a palladium(II) moiety, i.e., [Pd(Me$_2$ppz)]$^{2+}$, was coordinated to two oxygen atoms in a mono-vacant site of [PW$_{11}$O$_{39}$]$^{7-}$ with an asymmetric configuration, resulting in an overall $C_1$ symmetry (Fig. 7). This result was in good agreement with that of the single-crystal X-ray structural analysis of **Cs-1**. The $^{183}$W NMR measurement of **Cs-2** did not provide a good spectrum even in DMSO-$d_6$ owing to its low solubility.

The $^1$H NMR spectrum of **Cs-1** in D$_2$O displayed 10 signals at 4.03, 3.94, 3.77, 3.45, 2.57, 2.38, 2.33, 2.23, 2.15, and 2.03 ppm with 1:1:1:1:3:1:1:1:3:1 intensities, as shown in Fig. 8. The signals at 2.57 and 2.15 ppm could be assigned to the methyl groups of the *Me*$_2$ppz molecule, while the eight broad signals at 4.03, 3.94, 3.77, 3.45, 2.38, 2.33, 2.23, and 2.03 ppm were due to the eight non-equivalent hydrogen atoms in the two -C*H*$_2$-C*H*$_2$- groups. A similar $^1$H NMR spectrum was observed for **TMA-1**, as shown in Fig. S6a. The $^1$H NMR spectrum in D$_2$O of the starting complex PdCl$_2$(Me$_2$ppz) exhibited signals at 3.82, 2.53 and 2.46 ppm with 4:4:6 intensities, as shown in Fig. S6b.[17] The signals at 3.82 and 2.54 ppm were assigned to two -C*H*$_2$-C*H*$_2$- groups, while that at 2.46 ppm was ascribed to the two equivalent methyl groups. Thus, the coordination of [Pd(Me$_2$ppz)]$^{2+}$ to the mono-vacant site of the {PW$_{11}$O$_{39}$} unit led to the splitting of the $^1$H NMR signals of the Me$_2$ppz molecule, and these results corresponded to the formation of asymmetric polyoxoanion **1**.

Due to the low solubility of **Cs-1** in D$_2$O, the $^{13}$C NMR spectrum (Fig. 9) was also obtained with the potassium salt of **1**, as observed for $^{183}$W NMR spectrum. Six signals were observed at 49.77, 50.34, 61.31, 61.65, 63.22, and 63.48 ppm. The signals at 49.77 and 50.34 ppm could be assigned to the methyl groups of the *Me*$_2$ppz molecule, while the two sets of broad signals at 61.31 and 61.65 ppm as well as 63.22 and 63.48 ppm could be assigned to the four non-equivalent carbon atoms of the -C*H*$_2$-C*H*$_2$- groups of the Me$_2$ppz molecule. This was consistent with the $^1$H NMR spectra of **Cs-1** and **TMA-1**.
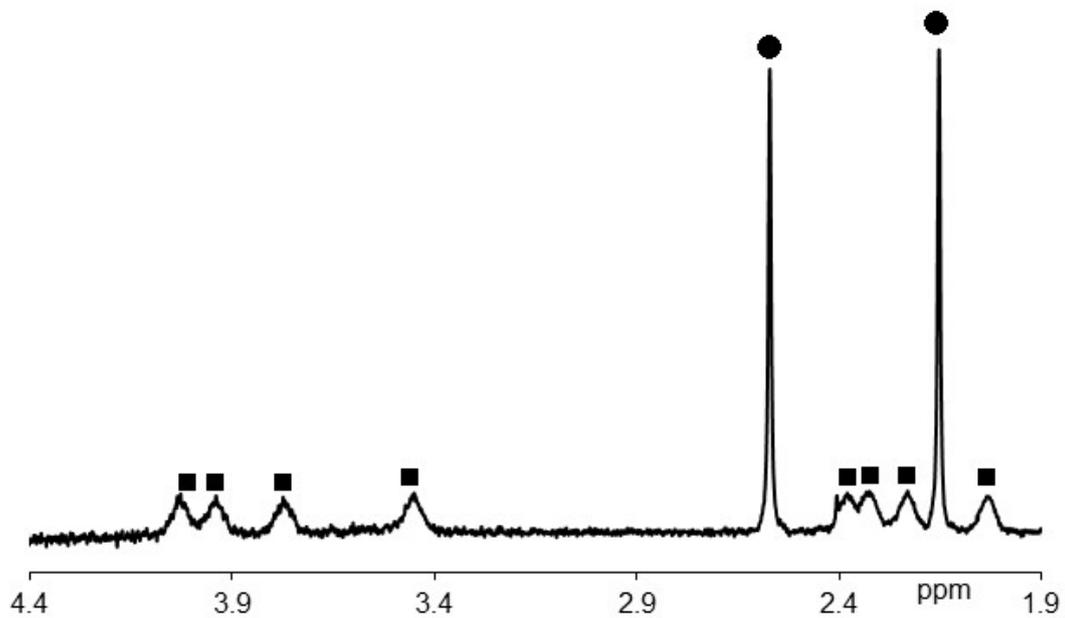
Figure 8. $^1$H NMR spectrum of **Cs-1** in D$_2$O.

The signals of the -C*H*$_2$-C*H*$_2$- (■) and methyl (●) groups of the Me$_2$ppz molecule were observed.
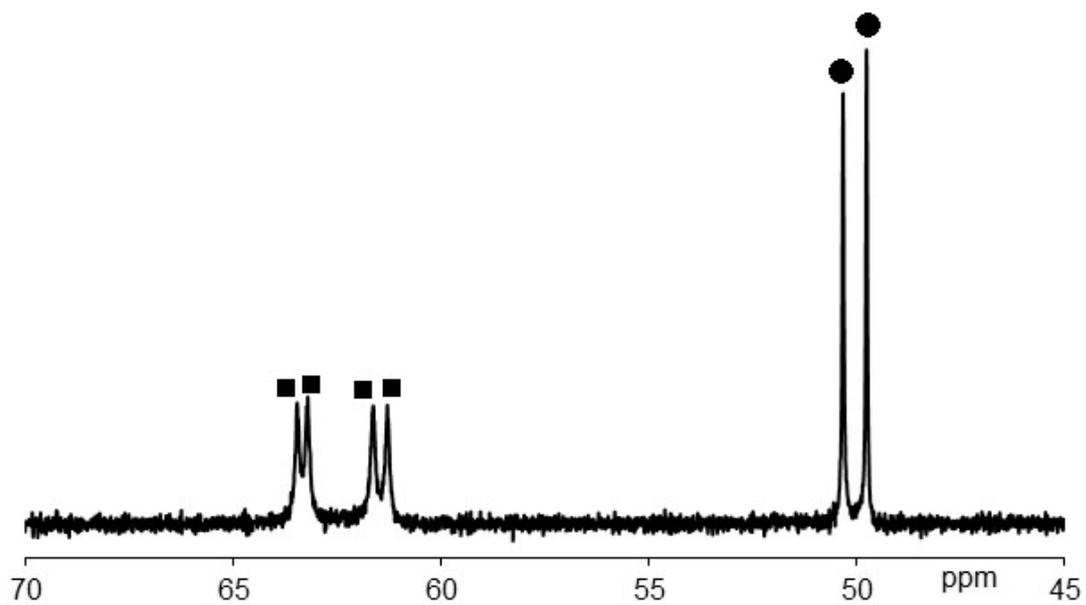
Figure 9. $^{13}$C NMR spectrum of the potassium salt of **1** in D$_2$O.

The signals of the -$C$H$_2$-$C$H$_2$- (■) and methyl (●) groups of the Me$_2$ppz molecule were observed.

The $^1$H NMR spectrum of **Cs-2** in DMSO-$d_6$ exhibited three broad signals at 5.52, 5.29, and 4.90 ppm with 1:2:1 intensities, as shown in Fig. 10. A set of signals at 5.52 and 4.90 ppm could be assigned to the two equatorial and two axial hydrogen atoms of the -C$H_2$-C$H_2$- groups, while a signal at 5.29 ppm was ascribed to the four equivalent hydrogen atoms of the -N$H_2$ groups of the ethylenediamine molecule. The $^1$H NMR spectrum in DMSO-$d_6$ of the starting complex PdCl$_2$(en) displayed two signals at 4.90 and 2.35 ppm with 1:1 intensities, which were assigned to the four equivalent hydrogen atoms of the two -C$H_2$-C$H_2$- groups and the four equivalent hydrogen atoms of the -N$H_2$ groups of the ethylenediamine molecule. These results also indicated that the two [Pd(en)]$^{2+}$ were symmetrically coordinated to the mono-vacant site of the {PW$_{11}$O$_{39}$} unit, as observed by X-ray crystallography.
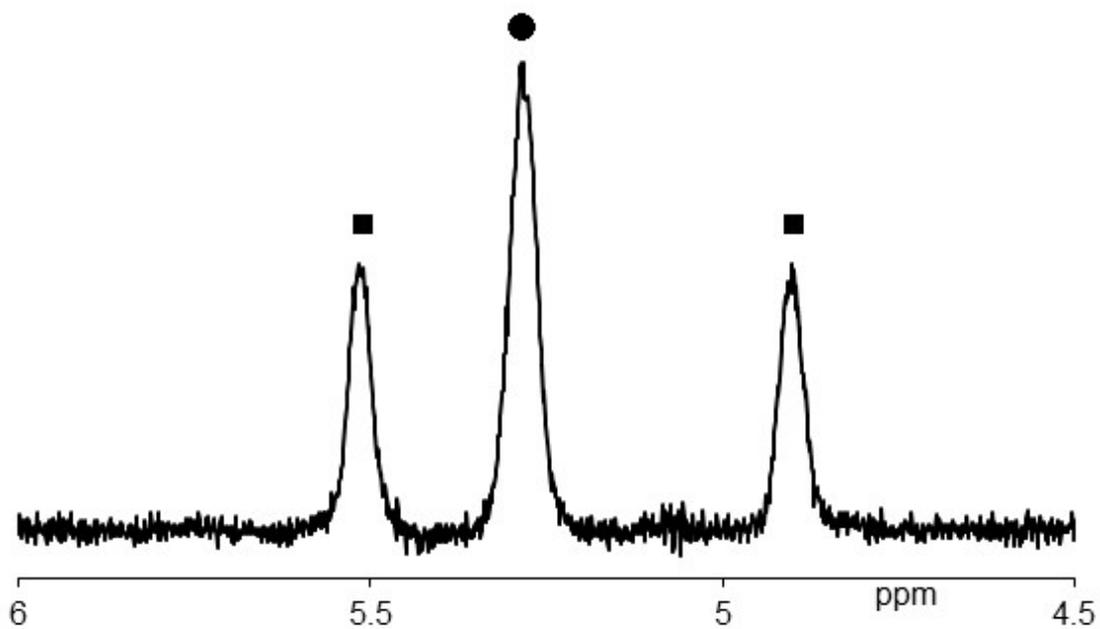
Figure 10. $^1$H NMR spectrum of **Cs-2** in DMSO-$d_6$.

The signals of the -C$H_2$-C$H_2$- (■) and –N$H_2$ (●) groups of two ethylenediamine molecules were observed.

The UV-Vis spectrum of **Cs-1** in water exhibited two broad absorption bands at 252 (extinction coefficient: $\varepsilon$ 38886 $M^{-1}cm^{-1}$) and around 387 nm ($\varepsilon$ 389 $M^{-1}cm^{-1}$) (Fig. S7). The broad band at approximately 252 nm could be assigned to the charge transfer (CT) bands of W-O. PdCl$_2$(Me$_2$ppz) displayed a band at 373 nm ($\varepsilon$ 494 $M^{-1}cm^{-1}$). Therefore, it was inferred that the absorption of **Cs-1** at around 387 nm derived from the [(Me$_2$ppz)Pd]$^{2+}$ species. **TMA-1** also displayed a similar absorption at 247 and around 393 nm (Fig. S8), suggesting that **TMA-1** possessed the same polyoxoanion structure as **Cs-1**. The UV-Vis spectrum of **Cs-2** was measured only at a low concentration because of its low solubility in water. As a result, a band at 252 nm ($\varepsilon$ 44174 $M^{-1}cm^{-1}$) deriving from W-O was observed, as shown in Fig. S9. This result supported the belief that **Cs-2** retained a Keggin-type structure, as observed for **Cs-1** and **TMA-1**.

**Structural transformation of the mono-lacunary $\alpha$-Keggin structure of Cs-1 to di-lacunary $\gamma$-Keggin polyoxotungstate, Cs$_7$[$\gamma$-PW$_{10}$O$_{36}$]**

As mentioned above, when cesium chloride was added to a mixture of Pd$^{II}$Cl$_2$(Me$_2$ppz) and [$\alpha$-PW$_{11}$O$_{39}$]$^{7-}$, Cs$_7$[$\gamma$-PW$_{10}$O$_{36}$] was formed as by-product. The FTIR and $^{31}$P NMR spectra in D$_2$O are shown in Figs. S10 and S11, respectively. The amount of Cs$_7$[$\gamma$-PW$_{10}$O$_{36}$] increased as the amount of added CsCl increased from 7.5 to 15 mmol, as shown in Fig. 11. Such a structural transformation was also observed for mono-platinum(II)-containing polyoxotungstate [$\alpha$-PW$_{11}$O$_{39}${Pt$^{II}$(Me$_2$ppz)}]$^{5-}$.[16] When 15 mmol or more of CsCl was added, a mono-lacunary $\alpha$-Keggin polyoxotungstate was formed. However, polyoxoanion **1** was hardly obtained as precipitate when 7.5 mmol or less of CsCl was added to the mixed solution. Moreover, Cs$_7$[$\gamma$-PW$_{10}$O$_{36}$] did not form when an excess of cesium chloride was added to an aqueous solution of **TMA-1**.

It was reported that the $\alpha$-isomer is generally favored for Keggin-type polyoxotungstates.[18,19] In the case of **Cs-2** and di-platinum(II)-containing $\alpha$-Keggin polyoxotungstate Cs$_3$[$\alpha$-PW$_{11}$O$_{39}${cis-Pt$^{II}$(NH$_3$)$_2$}$_2$] $\cdot$ 8H$_2$O, [20] Cs$_7$[$\gamma$-PW$_{10}$O$_{36}$] was not

produced even when an excess of cesium chloride was added. Since the formation of $Cs_7[\gamma$-$PW_{10}O_{36}]$ was not observed even when cesium chloride was added to $[\alpha$-$PW_{11}O_{39}]^{7-}$, a direct isomerization of $\alpha$ to $\gamma$ structures upon addition of cesium chloride could be observed only when a palladium(II) or platinum(II) species bearing *N,N'*-dimethylpiperazine as organic ligand was coordinated to the mono-lacunary Keggin-type polyoxotungstate in the presence of cesium ions. To the best of our knowledge, such unique structural transformations have never been reported so far for polyoxotungstates. The investigation of the mechanism of this transformation is in progress and will be reported elsewhere.
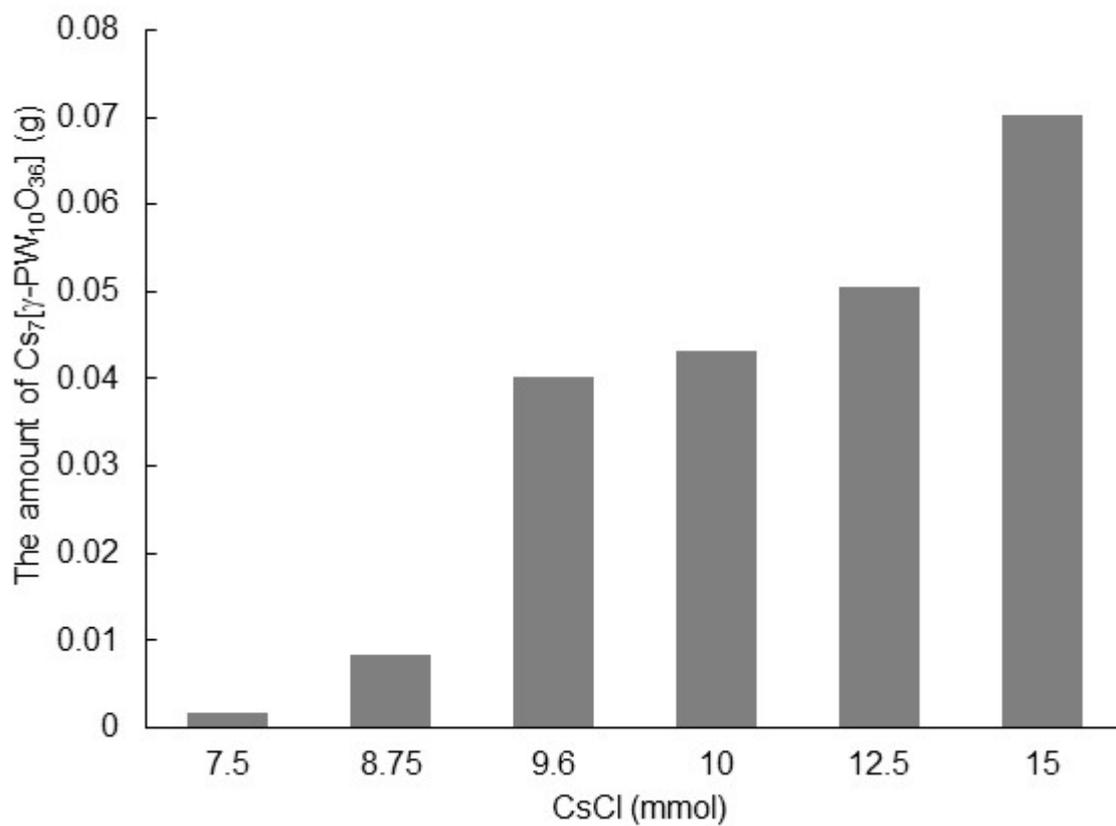
Figure 11. Plot of the amount of $Cs_7[\gamma\text{-}PW_{10}O_{36}]$ *vs*. number of moles of added CsCl

## Conclusion

Monomeric mono- and di-palladium(II) complexes composed of mono-lacunary $\alpha$-Keggin polyoxotungstates, i.e., $Cs_5[\alpha\text{-}PW_{11}O_{39}\{Pd^{II}(Me_2ppz)\}]\cdot 5H_2O$ (**Cs-1**), $[(CH_3)_4N]_4H[\alpha\text{-}PW_{11}O_{39}\{Pd^{II}(Me_2ppz)\}]\cdot 8H_2O$ (**TMA-1**), and $Cs_{2.5}H_{0.5}[\alpha\text{-}PW_{11}O_{39}\{Pd^{II}(en)\}_2]\cdot 7H_2O$ (**Cs-2**), were successfully synthesized. Their characterization was accomplished by X-ray structural analysis, elemental analysis, TG/DTA, FTIR, UV-Vis, and solution {$^1H$, $^{13}C$, $^{31}P$, and $^{183}W$} NMR spectroscopy.

Single-crystal X-ray structural analysis of **Cs-1** revealed that a palladium(II) moiety, i.e., $[Pd(Me_2ppz)]^{2+}$, was coordinated to two oxygen atoms in the mono-vacant site of $[PW_{11}O_{39}]^{7-}$ with an asymmetric configuration, thus resulting in an overall $C_1$ symmetry. In contrast, **Cs-2** exhibited a dinuclear palladium(II) structure formed upon coordination of two palladium species, ($[Pd(en)]^{2+}$) to two oxygen atoms in the mono-vacant site with a symmetric configuration, therefore resulting in an overall $C_s$ symmetry.

During the synthesis of **Cs-1**, a structural transformation from mono-lacunary $\alpha$-Keggin structure to the di-lacunary $\gamma$-Keggin polyoxotungstate $Cs_7[\gamma\text{-}PW_{10}O_{36}]$ was observed upon addition of cesium chloride. Such structural transformation was also observed for $[\alpha\text{-}PW_{11}O_{39}\{cis\text{-}Pt^{II}(Me_2ppz)\}]^{5-}$. However, no such phenomenon was observed during the syntheses of **Cs-2** and $Cs_3[\alpha\text{-}PW_{11}O_{39}\{cis\text{-}Pt^{II}(NH_3)_2\}_2]\cdot 8H_2O$. This reactivity was due to the coordination of palladium or platinum bearing $N,N'$-dimethylpiperazine as organic ligand to a Keggin-type polyoxotungstate.

## Experimental Section

**Materials:** $K_7[PW_{11}O_{39}]\cdot 13H_2O^{[15]}$ and $cis\text{-}PdCl_2(Me_2ppz)^{[17]}$ were prepared as described in the literature. The number of solvated water molecules was determined by TG/DTA. All reagents and solvents were obtained from commercial sources and used as received.

**Instrumentation/analytical procedures:** Elemental analysis was performed by Mikroanalytisches Labor Pascher (Remagen, Germany). Infrared spectra were recorded on a Perkin-Elmer Spectrum100 Fourier transform infrared (FTIR) spectrometer using KBr disks at approximately 25 °C in air. TG and DTA data were obtained using a Rigaku Thermo Plus EVO2 TG/DTA 81205Z instrument. TG/DTA measurements were performed in air with temperatures increase of 4 °C/min between 20 and 500 °C. The $^1$H (600.17 MHz), $^{13}$C (150.92 MHz), and $^{31}$P-{$^1$H} (242.95 MHz) nuclear magnetic resonance (NMR) spectra in solutions were recorded using 5-mm outer diameter tubes on a JEOL ECA-600 NMR spectrometer (Shizuoka University). $^1$H and $^{13}$C NMR spectra were measured in $D_2O$ with reference to an internal standard, i.e., 3-(trimethylsilyl)-1-propanesulfonic acid sodium salt (DSS). Chemical shifts are reported as positive for resonances downfield of DSS ($\delta$ 0). The $^{31}$P NMR spectra were measured in $D_2O$ with reference to an external standard constituted of 85% $H_3PO_4$ in a sealed capillary. Chemical shifts were reported as negative on the $\delta$ scale for the resonances upfield of $H_3PO_4$ ($\delta$ 0). The $^{183}$W NMR (25.00 MHz) spectrum was recorded in a tube with an outer diameter of 10 mm on a JEOL ECA-600 NMR spectrometer (Kyusyu University). The $^{183}$W NMR spectrum measured in $D_2O$ was referenced to an external standard constituted of a saturated $Na_2WO_4$-$D_2O$ solution (substitution method). Chemical shifts were reported as negative for the resonances upfield of $Na_2WO_4$ ($\delta$ 0). Ultraviolet-visible (UV-Vis) spectra were recorded on a Perkin-Elmer Spectrum Lambda 650 spectrophotometer.

**Synthesis of $Cs_5[\alpha$-$PW_{11}O_{39}${*cis*-$PdMe_2$ppz}]·$5H_2O$ (Cs-1):** Solid $K_7[\alpha$-$PW_{11}O_{39}]$·$13H_2O$ (1.269 g, 0.4 mmol) was added to a solution of $PdCl_2(Me_2$ppz) (0.1152 g, 0.4 mmol) in 60 mL of water at 50 °C. After stirring for three days at approximately 25 °C, solid cesium chloride (1.684 g, 10 mmol) was added, and the mixture was stirred for 24 h. Then, a yellow precipitate was collected using a membrane filter (JG 0.2 μm). At this stage, a crude product (1.108 g) was obtained. For purification, it was then dissolved in 40 mL of water at approximately 25 °C, and placed in an ice bath for 1 h. A white insoluble precipitate was formed and removed by a

membrane filter (JG 0.2 μm), and the filtrate was concentrated to ca. 15 mL using a rotary evaporator at 50 °C. The solution was allowed to stand in the refrigerator at approximately 5 °C for one day. A yellow precipitate was collected using a membrane filter (JG 0.2 μm) to yield 0.5447 g of product (the yield was calculated on the basis of [mol of **Cs-1**]/[mol of $K_7[PW_{11}O_{39}]\cdot 13H_2O] \times 100$ and was 37%). To obtain single crystals for X-ray crystallography, the obtained product (1.00 g) was dissolved in 20 mL of water at 50 °C and slowly evaporated at approximately 25 °C for one month. This product was soluble in water and DMSO, while being insoluble in methanol, ethanol, acetone, and diethyl ether. Elemental analysis results showed the following composition: C, 1.93; H, 0.67; N, 0.78; P, 0.86; Pd, 2.87; Cs, 17.90; K, <0.1%. Calculations for $Cs_5[\alpha\text{-}PW_{11}O_{39}\{Pd(Me_2ppz)\}]\cdot xH_2O$ (x = 5) = $C_6H_{24}Cs_5N_2O_{44}Pd_1P_1W_{11}$ (MW: 3652.41): C, 1.97; H, 0.66; N, 0.77; P, 0.85; Pd, 2.91; Cs, 18.19; K, 0%. TG/DTA analysis under atmospheric conditions showed a weight loss of 2.63% with an endothermic point at 62.1 °C observed below 89.8 °C (based on calculations, 2.47% corresponds to five water molecules). Additionally, a weight loss of 3.08% with an exothermic peak at 264.7 °C was observed within the temperature range from 98.2 to 431.1 °C corresponding to a $Me_2ppz$ molecule (calculated 3.13%). FTIR (KBr disk) results in the 1600–400 $cm^{-1}$ region showed the following bands: 1457w, 1092m, 1042m, 948s, 895m, 859m, 807s, 792s, 757s, 723s, and 508w $cm^{-1}$. The NMR results gave $^1H$ NMR ($D_2O$, 22.4 °C): δ 4.03 (-C*H*$_2$C*H*$_2$- groups in $Me_2ppz$), 3.94 (-C*H*$_2$C*H*$_2$-), 3.77 (-C*H*$_2$C*H*$_2$-), 3.45 (-C*H*$_2$C*H*$_2$-), 2.57 ((C*H*$_3$)$_2$ppz), 2.38 (-C*H*$_2$C*H*$_2$-), 2.33 (-C*H*$_2$C*H*$_2$-), 2.23 (-C*H*$_2$C*H*$_2$-), 2.15 ((C*H*$_3$)$_2$ppz), and 2.03 (-C*H*$_2$C*H*$_2$-); $^{31}P$ NMR ($D_2O$, 23.8 °C): δ −11.39. UV-Vis absorption (in $H_2O$, 4.65 × $10^{-6}$ M and 9.90 × $10^{-4}$ M) showed: $\lambda$ 252 nm ($\varepsilon$ 38886 $M^{-1}cm^{-1}$) and around 387 nm ($\varepsilon$ 389 $M^{-1}cm^{-1}$). Due to the low solubility of **Cs-1** in $D_2O$, the $^{13}C$ and $^{183}W$ NMR measurements were performed using a potassium salt of $[\alpha\text{-}PW_{11}O_{39}\{Pd^{II}(Me_2ppz)\}]^{5-}$. The potassium salt was obtained as follows: solid $K_7[\alpha\text{-}PW_{11}O_{39}]\cdot 13H_2O$ (0.4 mmol) was added to a solution of $PdCl_2(Me_2ppz)$ (0.4 mmol) in 60 mL of water at 50 °C. After stirring for three days at approximately 25 °C, ethanol (150 mL) was added, and a yellow precipitate was collected using a membrane filter (JG 0.2 μm). The $^{31}P$ NMR spectrum measured in $D_2O$ observed a single signal at −11.36 ppm,

showing the same chemical shift as **Cs-1**. ^{13}C NMR (D$_2$O, 25.6 °C): δ 49.77 ((*CH$_3$*)$_2$ppz), 50.34 ((*CH$_3$*)$_2$ppz), 61.31(-*CH$_2$CH$_2$*- groups in Me$_2$ppz), 61.65 (-*CH$_2$CH$_2$*-), 63.22 (-*CH$_2$CH$_2$*-), and 63.48 (-*CH$_2$CH$_2$*-); [183]W NMR (D$_2$O, 22.9 °C): −85.66, −90.00, −107.4, −108.3, −114.3, −115.5, −125.2, −134.4, −144.8, −150.7, and −192.1.

**Synthesis of [(CH$_3$)$_4$N]$_4$H[α-PW$_{11}$O$_{39}${PdMe$_2$ppz}]·8H$_2$O (TMA-1)**: Solid (CH$_3$)$_4$NCl (1.096 g, 10.0 mmol) was added to a mixed solution of K$_7$[α-PW$_{11}$O$_{39}$]·13H$_2$O and PdCl$_2$(Me$_2$ppz), as shown in the synthesis of **Cs-1**. After stirring for a day at approximately 25 °C, a yellow precipitate was collected using a membrane filter (JG 0.2 μm). At this stage, a crude product (0.8020 g) was obtained. For purification, it was dissolved in 40 mL of water at 50 °C, and stored in a refrigerator at approximately 5 °C overnight. A yellow precipitate was collected using a membrane filter (JG 0.2 μm) to yield 0.3056 g of product (the yield was calculated on the basis of [mol of **TMA-1**]/[mol of K$_7$[PW$_{11}$O$_{39}$]·13H$_2$O] × 100 and was 23%). This product was soluble in water and DMSO, while being insoluble in methanol, ethanol, acetone, and diethyl ether. Elemental analysis results showed the following composition: C, 7.84; H, 2.35; N, 2.58; P, 0.91; Pd, 3.11, W, 60.70; K, <0.1%. Calculations for [(CH$_3$)$_4$N]$_4$H[α-PW$_{11}$O$_{39}${Pt(Me$_2$ppz)}]·xH$_2$O (x = 8) = C$_{22}$H$_{79}$N$_6$O$_{47}$Pd$_1$P$_1$W$_{11}$ (MW: 3339.52): C, 7.91; H, 2.38; N, 2.52; P, 0.93; Pd, 3.19; W, 60.55; K, 0%. TG/DTA analysis under atmospheric conditions showed a weight loss of 3.60% without a clear endothermic point observed below 216.8 °C (based on calculations, 4.33% corresponds to eight water molecules). Additionally, a weight loss of 14.08% with exothermic peaks at 271.3 and 464.4 °C was observed in the temperature range from 228.8 to 494.4 °C corresponding to a Me$_2$ppz molecule and 4[(CH$_3$)$_4$N]$^+$ (calculated 12.44%). FTIR (KBr disk) results in the 1600 – 400 cm$^{-1}$ region showed the following bands: 1485m, 1453w, 1383w, 1084m, 1045m, 950s, 890m, 849m, 806s, 794s, 761s, 731s, and 512w cm$^{-1}$. The NMR results gave ^{1}H NMR (D$_2$O, 23.3 °C): δ 4.10 (-*CH$_2$CH$_2$*- groups in Me$_2$ppz), 3.99 (-*CH$_2$CH$_2$*-), 3.87 (-*CH$_2$CH$_2$*-), 3.69 (-*CH$_2$CH$_2$*-), 3.20 ([(*CH$_3$*)$_4$N]$^+$), 2.61 ((*CH$_3$*)$_2$ppz), 2.48 (-*CH$_2$CH$_2$*-), 2.31 (-*CH$_2$CH$_2$*-), 2.26 ((*CH$_3$*)$_2$ppz); [31]P

NMR ($D_2O$, 23.0 °C): δ −11.80. UV-Vis absorption (in $H_2O$, $5.09 \times 10^{-6}$ M and $1.00 \times 10^{-3}$ M) showed: $\lambda$ 247 nm ($\varepsilon$ 37601 $M^{-1}cm^{-1}$) and around 393 nm ($\varepsilon$ 413 $M^{-1}cm^{-1}$).

**Synthesis of $Cs_{2.5}H_{0.5}[\alpha\text{-}PW_{11}O_{39}\{Pd(en)\}_2]\cdot 7H_2O$ (Cs-2):** A solution of $PdCl_2(en)$ (0.048 g, 0.2 mmol) in 20 mL of water at 90 °C was added to a solution of $K_7[PW_{11}O_{39}]\cdot 13H_2O$ (0.319 g, 0.1 mmol) in 20 mL of water at approximately 25 °C. After stirring for 15 min at approximately 25 °C, solid CsCl (0.337 g, 2.0 mmol) was added and the reaction mixture was stirred overnight. Then, a yellow precipitate was collected using a membrane filter (JG 0.2 μm). At this stage, a crude product was obtained in 0.281 g yield. For purification, the crude product was dissolved in 50 mL of water at 90 °C, followed by filtration through a membrane filter (JG 0.2 μm). After standing at approximately 25 °C overnight, a yellow crystalline precipitate was collected using a membrane filter (JG 0.2 μm). The obtained product was 0.103 g (the yield calculated on the basis of [mol of **Cs-2**]/[mol of $K_7[PW_{11}O_{39}]\cdot 13H_2O$] × 100 was 30%). To obtain single crystals for X-ray crystallography, the obtained product (0.168 g) was dissolved in 70 mL of water at 90 °C and slowly evaporated at approximately 25 °C for 19 days. The obtained product was slightly soluble in water and DMSO, while being insoluble in methanol, ethanol, acetone, and diethyl ether. Elemental analysis results showed the following composition: C, 1.67; H, 1.18; N, 1.93; P, 0.87; Pd, 6.39; Cs, 9.32; K, <0.025%. Calculations for $Cs_{2.5}H_{0.5}[\alpha\text{-}PW_{11}O_{39}\{Pd(en)\}_2]\cdot xH_2O$ (x = 7) = $C_4H_{30.5}Cs_{2.5}N_4O_{46}Pd_2P_1W_{11}$ (MW: 3469.10): C, 1.38; H, 0.89; N, 1.62; P, 0.89; Pd, 6.14%; Cs, 9.58; K, 0%. TG/DTA analysis under atmospheric conditions showed a weight loss of 4.04% with an endothermic point at 90.3 °C observed in the temperature range from 51.1 to 131.8 °C; calculations showed 3.64% for seven water molecules. Additionally, a weight loss of 3.74% with an exothermic peak at 251.7 °C was observed in the temperature range from 166.6 to 339.0 °C; calculations showed two ethylenediamine molecules (calcd. 3.46%). FTIR (KBr disk) results in the 1600–400 $cm^{-1}$ region showed the following bands: 1454w, 1396w, 1363w, 1312w, 1293w, 1165w, 1154w, 1098m, 1048m, 976sh, 952s, 892m, 852s, 796s, 735s, and 551m $cm^{-1}$. NMR results gave $^1H$ NMR (DMSO-$d_6$, 24.0 °C): δ 4.90

(en), 5.29 (en), and 5.52 (en); $^{31}$P NMR: (DMSO-$d_6$, 24.1 °C): δ −12.42. UV-Vis absorption (in H$_2$O, 1.15 × 10$^{-5}$ M) showed: λ 255 nm (ε 44174 M$^{-1}$cm$^{-1}$).

**X-Ray crystallography:** A yellow block crystal of **Cs-1** (0.28 × 0.25 × 0.23 mm$^3$) or **Cs-2** (0.18 × 0.09 × 0.05 mm$^3$) was mounted on a MicroMount. The measurements were conducted using a Rigaku VariMax with an XtaLAB P200 diffractometer using multi-layer mirror-monochromated Mo Kα radiation (λ = 0.71073 Å) at 120 ± 1 K. Data were collected and processed using CrysAlisPro 1.171.40.39a (Rigaku OD, 2019) for Windows, and absorption correction was performed by the multi-scan method. Structural analysis was performed using Olex2 1.3 for Windows.[21] The structure was solved by olex2.solve 1.3[22] and refined by SHELXL 2018/3.[23] For the two palladium-coordinated polyoxoanions, 11 tungsten atoms, one or two palladium atoms, a phosphorus atom, two (or four) nitrogen atoms, six (or four) carbon atoms, and 39 oxygen atoms were clarified. The 5 and 2.5 cesium ions were also identified; however, the solvated water molecules could not be modeled due to the disorder of the atoms. Accordingly, the residual electron density was removed using the SQUEEZE routine in PLATON.[24]

**Crystal data for Cs-1.** C$_6$H$_{14}$Cs$_5$N$_2$O$_{39}$PPdW$_{11}$; M = 3562.46, *orthorhombic*, space group *F d d* 2 *(#43)*, a = 38.7878(5), b = 27.6703(3), c = 41.0914(5) Å, V = 44102.2(9) Å$^3$, Z = 32, $D_c$ = 4.292 g/cm$^3$, μ(Mo-Kα) 265.31 cm$^{-1}$. R1 = 0.0459 ($I > 2σ(I)$), w$R2$ = 0.1189 (for all data). GOF = 1.046 (86553 total reflections, 26663 unique reflections where $I > 2σ(I)$). The CCDC reference number 2056326 contains the supplementary crystallographic data for this study.

**Crystal data for Cs-2.** C$_4$H$_{16}$Cs$_{2.5}$N$_4$O$_{39}$PPd$_2$W$_{11}$; M = 3342.60, *monoclinic*, space group *P* 2$_1$/*m* *(#11)*, a = 13.1340(4), b = 16.5770(4), c = 13.3630(4) Å, $β$ = 101.100(3)º, V = 2855.00(14) Å$^3$, Z = 2, $D_c$ = 3.888 g/cm$^3$, μ(Mo-Kα) 243.49 cm$^{-1}$. R1 = 0.0391 ($I > 2σ(I)$), w$R2$ = 0.1140 (for all data). GOF = 1.051 (29548 total reflections, 7090 unique reflections where $I > 2σ(I)$).

The CCDC reference number 2056327 contains the supplementary crystallographic data for this study.

## Acknowledgements

# References

[1] N. V. Izarova, A. Banerjee, U. Kortz, *Inorg. Chem.* **2011**, *50*, 10379–10386.

[2] N. V. Izarova, M. T. Pope, U. Kortz, *Angew. Chem. Int. Ed.* **2012**, *51*, 9492–9510.

[3] N. V. Izarova, B. Santiago-Schübel, S. Willbold, W. Heβ, P. Kögerler, *Chem. Eur. J.* **2016**, *22*, 16052–16056.

[4] N. V. Izarova, R. I. Maksimovskaya, S. Willbold, P. Kögerler, *Inorg. Chem.* **2014**, *53*, 11778–11784.

[5] J. Gao, J. Yan, S. Beeg, D. Long, L. Cronin, *Angew. Chem. Int. Ed.* **2012**, *51*, 3373–3376.

[6] T. Hirano, K. Uehara, K. Kamata, N. Mizuno, *J. Am. Chem. Soc.* **2012**, *134*, 6425–6433.

[7] T. Hirano, K. Uehara, S. Uchida, M. Hibino, K. Kamata, N. Mizuno, *Inorg. Chem.* **2013**, *52*, 2662–2670.

[8] P. J. Domaille, G. Hervé, A. Tézé, *Inorg. Synth.* **27**, *1990*, 96–104.

[9] W. H. Knoth, R. L. Harlow, *J. Am. Chem. Soc.* **103**, *1981*, 1865–1867.

[10] I. D. Brown, D. Altermatt, *Acta Cryst.* **1985**, *B41*, 244–247

[11] I. D. Brown, R. D. Shannon, *Acta Cryst.* **1973**, *A29*, 266–282

[12] I. D. Brown, *Acta Cryst.* **1992**, *B48*, 553–572

[13] I. D. Brown, *J. App. Cryst.* **1996**, *29*, 479–480

[14] N. E. Brese, M. O'Keeffe, *Acta Cryst*. **1991**, *B47*, 192–197.

[15] R. Contant, *Can. J. Chem.* **1987**, *65*, 568–573.

[16] C. N. Kato, S. Nagatani, T. Mizuno, *Eur. J. Inorg. Chem.* **2019**, 517–522.

[17] F. G. Mann, H. R. Watson*, J. Chem. Soc.* **1958**, 2772–2780.

[18] I. A. Weinstock, J. J. Cowan, E. M. G. Barbuzzi, H. Zeng, C. L. Hill, *J. Am. Chem. Soc.* **1999**, *121*, 4608−4617.

[19] X. López, J. M. Maestre, C. Bo, J.-M. Poblet, *J. Am. Chem. Soc.* **2001**, *123*, 9571−9576.

[20] C. N. Kato, Y. Morii, S. Hattori, R. Nakayama, Y. Makino, H. Uno, *Dalton Trans.* **2012**, *41*, 10021–10027.

[21] O. V. Dolomanov, L. J. Bourhis, R. J. Gildea, J. A. K. Howard, H. Puschmann, *J. Appl. Cryst.* **2009**, *42*, 339-341.

[22] L. J. Bourhis, O.V. Dolomanov, R. J. Gildea, J. A. K. Howard, H. Puschmann, *Acta Cryst.* **2015**, *A71*, 59–75.

[23] G. M. Sheldrick, *Acta Cryst.* **2015**, *C71*, 3–8.

[24] A. L. Spek, *Acta Cryst.* **2009**, *D65*, 148–155.